Macromolecular Ligands for Gadolinium MRI Contrast Agents

ARTICLE *in* MACROMOLECULES · MAY 2012

Impact Factor: 5.8 · DOI: 10.1021/ma300521c

Macromolecules

Article

pubs.acs.org/Macromolecules

Macromolecular Ligands for Gadolinium MRI Contrast Agents

Yang Li,[†] Mariana Beija,[†] Sophie Laurent,[‡] Luce vander Elst,[‡] Robert N. Muller,[‡] Hien T. T. Duong,[†] Andrew B. Lowe,*[,§] Thomas P. Davis,*[,†] and Cyrille Boyer*[,†,§]

[†]Australian Centre for Nanomedicine (ACN), School of Chemical Engineering, The University of New South Wales, Sydney, NSW 2052, Australia

[‡]NMR and Molecular Imaging Laboratory, Department of General, Organic and Biomedical Chemistry, University of Mons, 7000 Mons, Belgium

[§]Centre for Advanced Macromolecular Design (CAMD), School of Chemical Engineering, University of New South Wales, Sydney NSW 2052, Australia

Supporting Information

ABSTRACT: Macromolecular ligands for gadolinium contrast agents (CAs) were prepared via a "grafting to" strategy. Copolymers of oligoethylene glycol methyl ether acrylate (OEGA) and an activated ester monomer, pentafluorophenyl acrylate (PFPA), were synthesized and modified with the 1-(5-amino-3-aza-2-oxypentyl)-4,7,10-tris(*tert*-butoxycarbonylmethyl)-1,4,7,10-tetraazacyclododecane (DO3A-*t*Bu-NH_2) chelate for the complexation of Gd^{3+}. The relaxivity properties of the ligated Gd^{3+} agents were then studied to evaluate the effect of macromolecular architecture on their behavior as magnetic resonance imaging (MRI) CAs. Ligands made from linear and hyperbranched macromolecules showed a substantially increased relaxivity in comparison to existing commercial Gd^{3+} MRI contrast agents. In contrast, star nanogel polymers exhibited a slightly lower relaxivity per Gd^{3+} ion (but still substantially higher relaxivity than existing low molecular weight commercial CAs). This work shows that macromolecular ligands have the potential to serve as components of Gd MRI agents as there are enhanced effects on relaxivity, allowing for lower Gd concentrations to achieve contrast, while potentially imparting control over pharmacokinetics.

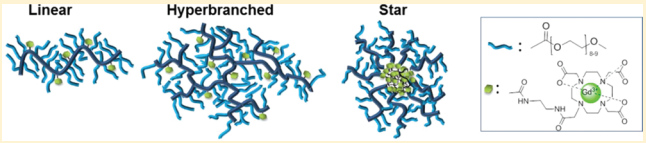

INTRODUCTION

Magnetic resonance imaging (MRI) is an indispensable clinical tool for the early detection of disease with widespread applications in cancer and cardiovascular diagnosis and treatment. MRI is a noninvasive technique, exhibiting excellent spatial and temporal resolution while obviating exposure to harmful radiation. The sensitivity of MRI to differences in tissue type is, nonetheless, relatively low, so contrast agents (CAs) are usually required to shorten the surrounding water protons longitudinal (T_1) and transversal (T_2) relaxation times to improve contrast. Two broad categories of CAs for MRI can be considered: (1) positive (or T_1) contrast agents that mainly shorten T_1 and give rise to image brightening, using mostly paramagnetic gadolinium based CAs[1] and (2) negative (or T_2) contrast agents that largely decrease T_2 and lead to image darkening with ferromagnetic iron nanoparticles being the most important example.[2] In approximately one-third of MRI scans, positive contrast agents based on low molecular weight Gd^{3+} chelates, namely Gd^{3+}-diethylenetriaminepentaacetic acid (Gd^{3+}-DTPA) or Gd^{3+}-tetraazacyclododecanetetraacetic acid (Gd^{3+}-DOTA), are administered to patients prior to or during the scanning procedure.[1c] Gd^{3+} is very efficient in catalytically shortening the relaxation times of bulk water protons as it possesses paramagnetic properties induced by seven unpaired electrons. However, commercial low molecular weight CAs have several shortcomings: (i) they rapidly extravasate from blood vessels to the interstitial space, making them inadequate for imaging cardiovascular systems; (ii) they have a short circulation time, precluding accumulation in tumors; (iii) they show poor contrast at high magnetic fields; and (iv) they are only effective at high concentrations (>0.1 mM), causing problems with Gd^{3+} leakage and/or accumulation that can (in a small minority of cases) cause nephrogenic systemic fibrosis.[3]

The purpose of the present work is to investigate the potential benefits that might be gained by incorporating Gd^{3+} within macromolecular structures, by potentially tuning relaxivity and/or pharmacokinetics.[4] The combined effect of increasing the number of Gd^{3+} atoms per molecule and reducing molecular tumbling[5] has been shown to lead to a significant shortening of relaxation times and, consequently, an enhancement of contrast (potentially permitting reduced clinical dosing). Conjugation of imaging agents to biocompatible polymers (e.g., poly(ethylene oxide)) should lead to longer blood circulation times, promoting accumulation in tumors by the enhanced permeation and retention (EPR) effect. The favored chelating group for Gd^{3+} is 1,4,7-tris-(carboxymethylaza)cyclododecane-10-azaacetylamide (DO3A) and we used this as a starting point in our work as DO3A is

Received: March 14, 2012
Revised: April 22, 2012
Published: May 9, 2012

relatively similar to DOTA, a well-used chelating agent for gadolinium complexation (and is already approved by the FDA).[6] Potentially, a macromolecular ligand structure also provides a scaffold to allow inclusion of tissue-specific targeting moieties (multiple sites favoring the multiligand effect), which could be used to enhance Gd^{3+} concentration at diseased tissue sites. Previously, Gd^{3+} chelates have been covalently bound to biocompatible linear polymers (e.g., poly(lysine)[7] or poly(*N*-(2-hydroxypropyl)methacrylamide[8]) and also complex structures such as block copolymer micelles[9] and dendrimers.[10] In very recent work, a polymeric CA based on a star architecture was reported in the literature,[11] where catechol chelates were attached to the arms of stars yielding CAs with a very high relaxivity (84 mM^{-1} s^{-1}). However, we have been unable to find any published studies on the use of star carriers with Gd^{3+} within their cores.

Poly(ethylene oxide)-based polymers are particularly interesting as ligand components as they are nontoxic and antifouling.[12] Recently, Grogna et al. prepared linear copolymers of oligoethylene glycol methyl ether acrylate (OEGA) grafted with a Gd^{3+} DOTA-like chelate, 2,2′,2″-(1,4,7,10-tetraazacyclododecane-1,4,7-triyl) triacetate monoamide (DO3A-MA), using either a "grafting through"[13] or a "grafting to"[14] approach and studied the influence of the rigidity of the spacer on relaxivity.

Our interest in MRI agents started with the design of iron oxide magnetic nanoparticles for theranostics,[15] and we have now expanded our work to the development of macromolecular positive contrast agents based on Gd^{3+}. In the present work, we studied the effect of three different polymer architectures—linear, hyperbranched (hbp), and star—on the relaxivity properties of macromolecular CAs. We hypothesized that a globular nanostructure might promote an improvement in contrast efficiency by inducing a synergistic effect of high local Gd^{3+} concentrations and a simultaneous reduction in tumbling from polymer-imposed restriction of movement. Hyperbranched polymers, simple analogues of dendrimers (with greater macromolecular heterogeneity), have attracted minimal prior interest as components in MRI CA formulations.[16]

EXPERIMENTAL SECTION

Materials. Oligo(ethylene glycol) methyl ether acrylate (480 g mol^{-1}, 99%, OEGA), trifluoroacetic acid (99%), *n*-butanethiol (99%), *N,N*′-bis(acryloyl)cystamine (>97%), 2-hydroxyethyl disulfide, 2-bromopropionyl bromide (97%), 3-mercaptopropionic acid (≥99%), carbon disulfide (99%+), and gadolinium (III) nitrate hexahydrate (99.99%) were purchased from Aldrich and used as received. 3-(Trimethylsilyl)-2-propyn-1-ol (97%) was purchased from Lancaster. Pentafluorophenyl acrylate (PFPA)[17] and 3-(benzylsulfanylthiocarbonylsulfanyl)propionic acid (BSPA)[18] were synthesized according to previously reported procedures. 2,2′-Azobis(isobutyronitrile) (AIBN, Wako Chemicals) was crystallized twice from methanol before use. 1-(5-Amino-3-aza-2-oxpentyl)-4,7,10-tris(*tert*-butoxycarbonylmethyl)-1,4,7,10-tetraazacyclododecane (DO3A-*t*-Bu-NH_2, >94%) was purchased from Macrocyclics (Dallas, TX) and used as received. Acetonitrile, toluene, triethylamine, and dichloromethane were used without further purification. High-purity N_2 (Linde gases) was used for degassing. Membranes for dialysis (MWCO 3500 Da) were purchased from Fisher Biotec (Cellu SepT4, regenerated cellulose tubular membrane).

Syntheses. *Synthesis of 3-(Trimethylsilyl)prop-2-yn-1-yl 2-Bromopropanoate.* Triethylamine (4.1 g, 41 mmol) was added dropwise to a stirring solution of 3-(trimethylsilyl)-2-propyn-1-ol (5 g, 39 mmol) in dichloromethane (DCM, 50 mL), all cooled in an ice bath. After stirring for 30 min, a solution of 2-bromopropionyl bromide (8.84 g, 41 mmol) in DCM (10 mL) was added dropwise. The resulting solution was stirred overnight at room temperature. The mixture was then washed with brine, and the organic phase was collected and dried over anhydrous magnesium sulfate. The solvent was removed by rotary evaporation and further dried in vacuum oven at room temperature overnight, yielding a brown liquid. Yield 9.33 g (86.5%). Figures S1 and S2 in the Supporting Information show the ^1H and ^{13}C NMR spectra of 3-(trimethylsilyl)prop-2-yn-1-yl 2-bromopropanoate. ^1H NMR (300 MHz, $CDCl_3$): δ 5.08 (d, J = 19.4 Hz, 2H), 4.82 (q, 2H), 1.95 (d, 3H), 0.08 (s, 9H). ^{13}C NMR (75 MHz, $CDCl_3$): δ 172.4, 111.6, 100.2, 57.8, 39.7, 19.5, 2.0.

Synthesis of 3-(Trimethylsilyl)prop-2-yn-1-yl 2-((((3-Propionic acid)thio)carbonothioyl)thio)propanoate) (TSPPA). Triethylamine (4 g, 40 mmol) was added dropwise to a stirred solution of 3-mercaptopropionic acid (2 g, 19 mmol) and carbon disulfide (2.2 g, 29 mmol) in dichloromethane (DCM, 50 mL). The solution was left to stir at room temperature for 2 h, and then a solution of 3-(trimethylsilyl)prop-2-yn-1-yl 2-bromopropanoate (5 g, 19 mmol) in DCM (30 mL) was added dropwise. The resulting solution was stirred overnight at room temperature. The final mixture was washed with a 0.1 M HCl aqueous solution (5 × 250 mL). Subsequently, the solvent was removed by rotary evaporation, and the product was purified by column chromatography using a mixture of ethyl acetate/petroleum spirit as eluent (1/20 v/v). The product was isolated by evaporation of solvent and further dried in a vacuum oven at room temperature overnight to yield a yellow oil. Yield 4.38 g (72%). Figures S3 and S4 in the Supporting Information show the ^1H and ^{13}C NMR spectra of 3-(trimethylsilyl)prop-2-yn-1-yl 2-((((3-propionic acid)thio)-carbonothioyl)thio)propanoate). ^1H NMR (300 MHz, $CDCl_3$): δ 5.09 (s, 2H), 4.32 (q, 1H), 3.28 (t, 2H), 2.85 (t, 2H), 1.50 (d, 3H), 0.08 (s, 9H). ^{13}C NMR (75 MHz, $CDCl_3$): δ 228.03, 175.03, 172.54, 111.65, 57.86, 57.58, 41.91, 34.14, 27.99, 16.22, −1.96.

Synthesis of the Cross-Linker Disulfanediylbis(ethane-2,1-diyl) Diacrylate. 2-Hydroxyethyl disulfide (5 g, 3.97 mL, 32 mmol) and anhydrous dichloromethane (50 mL) were added into a 250 mL round bottom flask equipped with a magnetic stir bar in an ice bath. A solution of triethylamine (6.88 g, 9.42 mL, 68 mmol) in dichloromethane (10 mL) was added to the mixture. After stirring for 30 min, a solution of acryloyl choride (6.15 g, 5.5 mL, 68 mmol) in dichloromethane (10 mL) was then added dropwise. The mixture was then stirred overnight at room temperature. The solution was extracted using 250 mL of 0.1 M hydrochloric acid five times. The organic layers were combined, and solvent was removed by evaporation. The product was purified by chromatography through a silica column using a mixture of ethyl acetate/petroleum spirit (1/10 v/v) as eluent. The product was isolated by evaporation of the solvent and further dried in a vacuum oven at room temperature overnight, yielding a light brown liquid. Yield 4.38 g (52%). Figures S5 and S6 in the Supporting Information show the ^1H and ^{13}C NMR spectra of cross-linker disulfanediylbis(ethane-2,1-diyl) diacrylate. ^1H NMR (300 MHz, $CDCl_3$): δ 6.41 (d, 1H), 6.12 (q, 1H), 5.83 (d, 1H), 4.03 (t, 2H), 2.84 (t, 2H). ^{13}C NMR (75 MHz, $CDCl_3$): δ 168.90, 129.54, 127.80, 62.98, 39.01.

Synthesis of Linear P(OEGA-stat-PFPA). OEGA (5 g, 11 mmol), PFPA (285 mg, 1.1 mmol), BSPA (64 mg, 0.24 mmol), and AIBN (7.7 mg, 0.047 mmol) were dissolved in acetonitrile (7 mL). The mixture was degassed by purging with N_2 for 30 min at 0 °C and then placed in an oil bath at 65 °C. The polymerization was conducted for 6 h and then interrupted by cooling the mixture in an ice bath and exposing it to air. Monomer conversion was determined by ^1H and ^{19}F NMR and size exclusion chromatography (SEC) analysis was undertaken to assess molecular weight distribution. The polymer was purified by repeated precipitations in diethyl ether and then dried under vacuum. The final composition determined by ^1H NMR and ^{19}F NMR is equal to 83/17 mol % in OEGA and PFPA.

Synthesis of Hyperbranched P(OEGA-co-PFPA). OEGA (5 g, 4.59 mL, 10 mmol), PFPA (620 mg, 2.6 mmol), disulfanediylbis(ethane-2,1-diyl) diacrylate (340 mg, 1.29 mmol), TSPPA (250 mg, 0.78 mmol), and AIBN (8.5 mg, 0.052 mmol) were dissolved in acetonitrile (13 mL), and the mixture was purged with N_2 for 30 min at 0 °C. The

dx.doi.org/10.1021/ma300521c | *Macromolecules* 2012, 45, 4196−4204

solution was stirred at 60 °C for 12 h, and the polymerization was then stopped by cooling it in an ice bath. Samples were extracted for determination of monomer conversion by ^{1}H and ^{19}F NMR and molecular weight by SEC. The polymer was purified by repeated precipitations in cold diethyl ether and then dried under vacuum. ^{1}H NMR and ^{19}F NMR spectra of hyperbranched polymers are shown in Figures S7 and S8. The final composition of the 93.2/6.8 mol % in OEGA/PFPA.

Synthesis of Star POEGA-b-P(PFPA-co-(N,N-bis(acryloyl)-cystamine)) via an Arm-First Methodology. First, poly(oligo-(ethylene glycol) methyl ether acrylate) (POEGA) homopolymer arms were synthesized. Briefly, OEGA (1 g, 2 mmol), 3-(trimethylsilyl)prop-2-yn-1-yl 2-((((3-propionic acid)thio)-carbonothioyl)thio)propanoate) (TSPPA, 18 mg, 48 μmol), AIBN (0.8 mg, 4.8 μmol), and acetonitrile (2 mL) were placed in a vial equipped with a magnetic stir bar. The mixture was degassed by purging with N_2 for 30 min at 0 °C. The polymerization was carried out at 60 °C for 12 h prior to cessation by cooling and exposure to air. Monomer conversions were determined by ^{1}H NMR (70% monomer conversion after 12 h), and the molecular weights were assessed by SEC and by ^{1}H NMR spectroscopy (Figure S9 in the Supporting Information). The polymer was isolated by precipitation in diethyl ether and dried under vacuum.

To make the star copolymer, POEGA (0.5 g, 0.03 mmol, M_n = 16 000 g mol^{-1}, $Đ$ = 1.16), PFPA monomer (37.2 mg, 0.16 mmol), *N,N*-bis(acryloyl)cystamine (65 mg, 0.24 mmol), AIBN (0.5 mg, 0.003 mmol), and toluene (5 mL) were charged to a vial equipped with a magnetic stirrer. The mixture was purged with N_2 for 30 min at 0 °C, and then the polymerization was carried out at 70 °C for 24 h. After the polymerization, the vials were immediately cooled in an ice bath and the contents exposed to air. The polymer was purified by precipitation in diethyl ether and then dried under vacuum. The polymer was also dialyzed using a membrane with a molecular weight cutoff 50 000 Da for 3 days against acetone. ^{1}H and ^{19}F NMR spectra are shown in Figures S10 and S11.

Chemical Modification with DO3A-tBu-NH$_2$ Chelate and Deprotection. A typical procedure for the chemical modification of P(OEGA-*co*-PFPA) polymers with DO3A-*t*Bu-NH$_2$ is as follows: P(OEGA-*stat*-PFPA) (1.1 g, 0.35 mmol of PFPA moieties) was dissolved in DMF (5 mL). DO3A-*t*Bu-NH$_2$ (355 mg, 0.5 mmol) and triethylamine (100 μL, 0.7 mmol) were added, and the mixture was stirred for 48 h. A sample was taken, and ^{19}F NMR was performed, showing that all PFPA moieties had reacted (Figure S13). The polymer was purified by several precipitations in diethyl ether and then analyzed by ^{1}H NMR spectroscopy (Figure S12). The solvent was evaporated, trifluoroacetic acid (TFA, 3 mL) was added, and the reaction was carried out overnight at room temperature. Then, unreacted TFA was removed by evaporation and the polymer was further purified by dialysis against water for 4 days. The polymer [P(OEGA-*co*-DO3A-MA)] was recovered as a yellowish tacky solid after freeze-drying. ^{1}H NMR and ^{19}F NMR spectra are reported in the Supporting Information (see Figures S12−S18).

Complexation with Gd^{3+}. P(OEGA-*co*-DO3A-MA) was dissolved in water, the pH was adjusted to 6, and the solution was heated at 60 °C for 1 h. Gd(NO$_3$)$_3$·6H$_2$O (1.5 equiv) was added, the pH was adjusted to 8, and the mixture was stirred for 48 h at room temperature. DOTA was then added to the aqueous solution to remove unreacted Gd^{3+} ions; the polymer was dialyzed against water for 5 days and freeze-dried. The final Gd^{3+} content was assessed by inductively plasma coupled optical emission spectrometry (ICP-OES).

Analyses. *NMR Spectroscopy.* Monomers conversions and polymer compositions were assessed by ^{1}H and ^{19}F NMR using a Bruker AC300F (300 MHz) spectrometer or a Bruker DPX300 (300 MHz) spectrometer.

OEG-A conversion was calculated using the equation

$$\alpha^{\mathrm{OEGA}} = \left(\int I^{\mathrm{CH{=}CH_2,5.5-6.5\ ppm}} / \int I^{\mathrm{OCH_3,3.6\ ppm}}\right) \times 100$$

where $\int I^{\mathrm{CH{=}CH_2,5.5-6.5\ ppm}}$ and $\int I^{\mathrm{OCH_3,3.3\ ppm}}$ correspond to intensities from acrylate bond of OEG-A and methyl ether.

PFPA conversion was calculated using ^{19}F NMR analysis and the equation

$$\alpha^{\mathrm{PEPAA}} = \left[\int^{-158.0\ \mathrm{ppm}} / \left(\int^{-158.0\ \mathrm{ppm}} + \int^{-152.5\ \mathrm{ppm}}\right)\right] \times 100$$

Size Exclusion Chromatography (SEC). SEC analyses of polymer samples were performed in *N,N*-dimethylacetamide (DMAc with 0.03% w/v LiBr and 0.05% 2,6-dibutyl-4-methylphenol (BHT) using a Shimadzu modular system comprising a DGU-12A degasser, an SIL-10AD automatic injector, and a 5.0 μm bead-size guard column (50 × 7.8 mm) followed by four 300 × 7.8 mm linear Phenogel columns (bead size: a 5.0 μm; pore sizes: 10^5, 10^4, 10^3, and 500 Å) and an RID-10A differential refractive-index detector. The temperature of columns was maintained at 50 °C using a CTO-10A oven, and the flow rate was kept at 1 mL min^{-1} using a LC-10AT pump. A molecular weight calibration curve was produced using commercial narrow molecular weight distribution polystyrene standards with molecular weights ranging from 500 to 10^6 g mol^{-1}. Polymer solutions at 2−3 mg mL^{-1} were prepared in the eluent and filtered through 0.45 μm filters prior to injection.

Dynamic Light Scattering (DLS). DLS measurements were performed using a Malvern Zetasizer Nano Series running DTS software and using a 4 mW He−Ne laser operating at a wavelength of 633 nm and an avalanche photodiode (APD) detector. The scattered light was detected at an angle of 173°. The temperature was stabilized to ±0.1 °C of the set temperature. Aqueous solutions of polymer samples were filtered through a 0.45 μm pore size filter to remove dust prior to measurement. To assess size distributions, the autocorrelation function was fitted using the cumulants method.

Transmission Electron Microscopy (TEM). The sizes and morphologies of the star polymers were observed using a transmission electron microscopy JEOL1400 TEM at an accelerating voltage of 100 kV. The star polymer was dissolved in water (5 mg mL^{-1}) according to the solubility of the material and deposited onto 200 mesh, holey film, copper grid (ProSciTech). Osmium vapor (OsO_4) staining was applied.

Indutively Coupled Plasma−Optical Emission Spectrometry (ICP-OES). Gd^{3+} content of the macromolecular CAs was determined by inductively coupled plasma−optical emission spectrometry (ICP-OES) using a Perkin-Elmer OPTIMA 7300 spectrometer. Samples were prepared by dissolving 0.5 mg of polymer in 10 mL of ultrapure water.

Relaxivity Measurements. ^{1}H NMRD curves (nuclear magnetic resonance dispersion) of the macromolecular CAs were obtained at 310 K on a Stelar fast cycling relaxometer (PV, Mede, Italy) over a range of magnetic fields extending from 0.25 mM to 0.94 T (0.01−40 MHz). Measurements of T_1 and T_2 relaxation times were performed at 310 K on Minispec Mq-20 and Mq-60 (Bruker, Karlsruhe, Germany) working at 20 MHz (0.47 T) and 60 MHz (1.4 T), respectively.

Cell Culture. NIH 3T3 fibroblast cells were cultured in growth media consisting of Dulbecco's modified Eagle's medium:Nutrient Mix F-12 (DMEM) supplemented with 10% (v/v) fetal bovine serum (FBS) in a ventilated tissue culture flask T-75 and passaged every 2−3 days when monolayers at around 80% confluence. The cells were used only when stable cell growth was obtained (approximately 3−4 passages). The cells were incubated at 37 °C in a 5% CO_2 humidified atmosphere. The cell density was determined by counting the number of viable cells using a trypan blue dye (Sigma-Aldrich) exclusion test. The cells were detached using 0.05% trypsin−EDTA (Invitrogen), stained using trypan blue dye, and loaded on the hemocytometer. One day prior to the treatment, the cells were seeded at required cell densities on and 96-well plates.

Cell Viability. The cytotoxicity of prepared polymers was tested in vitro by a standard Alamar Blue assay, which provides a homogeneous, fluorescent method for monitoring cell viability. The assay is based on the ability of living cells to convert a redox dye (blue resazurin) into a fluorescent end product (red resorufin). Nonviable cells rapidly lose metabolic capacity and thus do not generate a fluorescent signal. The cells were seeded in a tissue culture treated 96-well plate in 100 μL medium per well at a density of 5000 cells/well and incubated for 24 h.

Scheme 1. Schematic Representation To Prepare Different Polymers Architectures

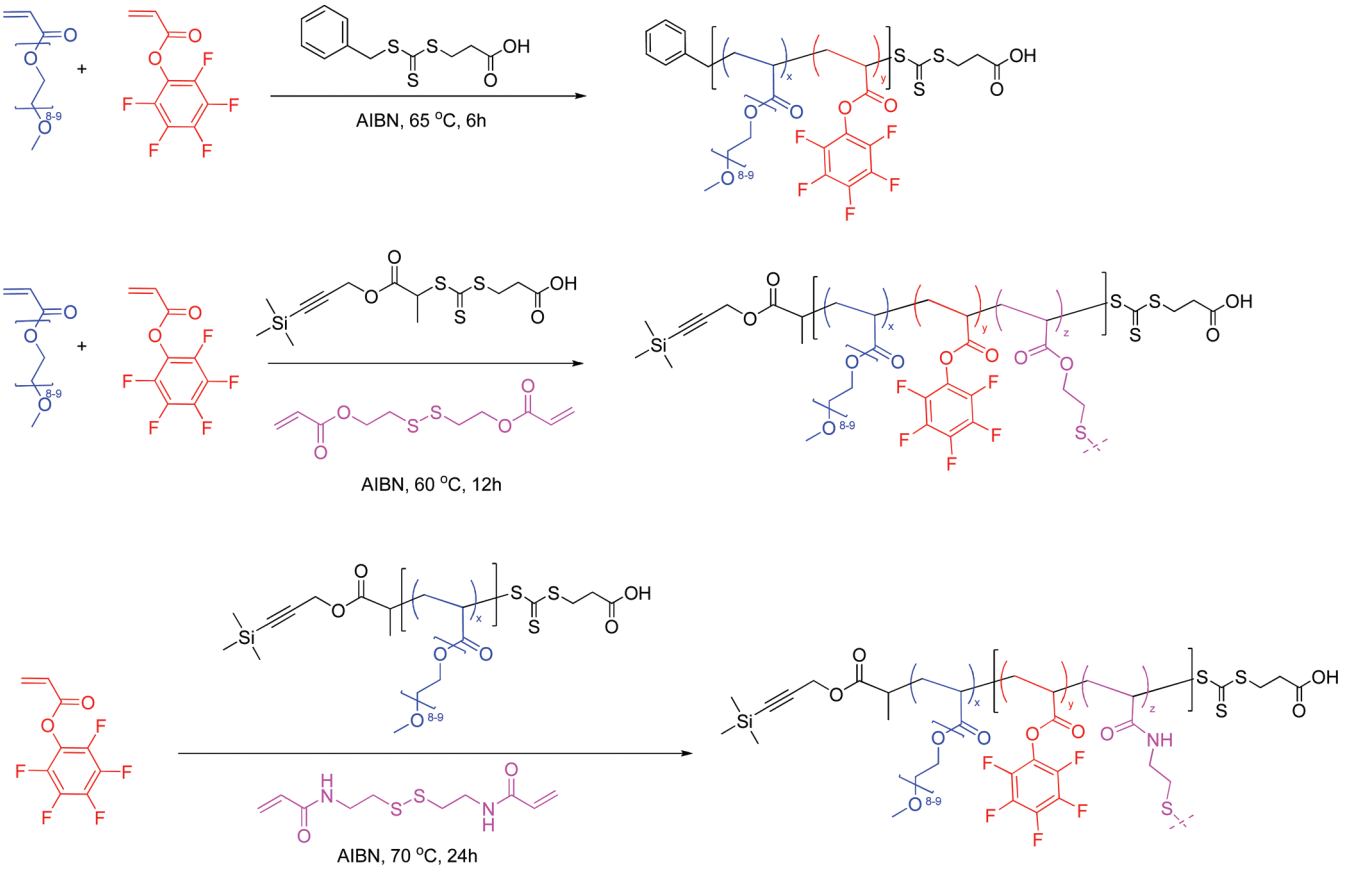

The medium was then replaced with fresh medium containing free Gd^{3+}, DOTA-star, or DOTA-hyperbranched polymer and Gd^{3+}-DOTA star or hyperbranched complexes over an equivalent concentration range of 25, 50, 200, 500, and 1000 μM based on Gd^{3+} and incubated for 72 h. Alamar Blue assay dye (20 μL) was then added to each well, and the cells were incubated for 5 h. After an incubation step, data were recorded using a fluorescence plate reader (570ex/595em). Cell viability was determined as a percentage of untreated control cells, and IC_{50} values were calculated via regression analysis using Microsoft Excel.

The amount of fluorescence produced (F) was proportional to the number of metabolically active (viable) cells in the culture. Wells without cells was set up as the negative control for the determination of background fluorescence. Wells without polymer treatment were used as the positive control. The cell viability was calculated by comparing the fluorescence products of treated and nontreated cells according to the equation

$$\text{cell viability (\%)} = \left(\frac{\overline{F}_{\text{sample}} - \overline{F}_{\text{negative control}}}{\overline{F}_{\text{positive control}} - \overline{F}_{\text{negative control}}} \right) \times 100\%$$

where $\overline{F}_{\text{sample}}$ is the average fluorescence product in the sample wells (cell treated with prepared polymer), $\overline{F}_{\text{negative control}}$ is the average fluorescence product in the negative control wells (without cells), and $\overline{F}_{\text{positive control}}$ is the average fluorescence product in the positive control wells (no treatment with polymers).

RESULTS AND DISCUSSION

Macromolecular CAs were prepared by postmodification of copolymers via reaction with an activated ester and amino chelating agent (DO3A), followed by complexation with Gd^{3+}. Statistical copolymers of oligoethylene glycol methyl ether acrylate (OEGA) and an activated ester monomer, pentafluorophenyl acrylate (PFPA), were synthesized using reversible addition−fragmentation chain transfer (RAFT) polymerization.[19] Pentafluorophenyl activated ester functionality was used as it has a higher solubility than poly(*N*-acryloxysuccinimide) while presenting a comparable reactivity toward amines.[20] We recently reported the successful modification of PFPA in the cores of star polymers using bulky amines such as galactosamine to give yields higher than 94%.[21] We therefore predicted that the PFPA/amine click reaction would be a good approach to attach relatively bulky amine-functional ligands for Gd^{3+} complexation to star cores.

Synthesis of Different Macromolecular Architectures via RAFT Polymerization. *Synthesis of Linear P(OEGA-co-PFPA) Copolymers (Scheme 1)*: For the linear architecture (Scheme 1), a statistical copolymerization with 90 mol % OEGA and 10 mol % PFPA was carried out at 65 °C for 6 h using 3-benzylsulfanylthiocarbonylsulfanylpropionic acid (BSPA) as the chain transfer agent (CTA) and AIBN as the initiator. A partial conversion of 83% in OEGA and 94% in PFPA was obtained, yielding a total conversion of 87% (Figure S19). ^{1}H NMR and ^{19}F NMR spectroscopies were employed to determine the composition of the copolymers (see Figure S20). ^{19}F NMR analysis confirms the incorporation of PFPA in the copolymers by the characteristic signal of the pentafluorophenyl ester at −152, −157, and −162 ppm. A slight compositional drift was observed in the copolymerization, with a higher concentration of PFPA moieties closer to the α-end (Figure S21). The polymerization was well controlled as evidenced by the experimental M_n being close to the theoretical value ($M_{n,\text{theor}}$ = 19 000 g mol^{-1}, calculated by the equation M_n = ($\alpha^{\text{OEGA}} \times [\text{OEGA}]_0/[\text{RAFT}]_0 \times M_w^{\text{OEGA}} + (\alpha^{\text{PFPA}} \times [\text{PFPA}]_0/$

dx.doi.org/10.1021/ma300521c | *Macromolecules* 2012, 45, 4196−4204

Table 1. Molecular Weights, Dispersities and Relaxivities of the Macromolecular CAs Used in This Study

architecture	M_n[a] [g mol^{-1}]	M_w/M_n[a]	Gd content[b] [wt %]	N^{Gd}[c]	ionic r_1[d] [mM^{-1} s^{-1}]	molecular r_1[e] [mM^{-1} s^{-1}]
Gd/DO3A	558		26.2	1	5.2	5.2
linear	18 700	1.21	5.7	6.8	15.6	106.1
hyperbranched	22 600	1.41	2.4	3.4	15.4	52.4
star	93 000	1.12	6.2	37	13.5	500

[a]Determined by SEC in DMAc using PS standards. [b]Determined by ICP-OES. [c]Number of gadolinium per macromolecules (N^{Gd}) calculated by N^{Gd} = ([Gd content]/M_w^{Gd})/([polymer content]/$M_n^{Polymer}$), where Gd content, M_w^{Gd}, and $M_n^{Polymer}$ correspond to Gd content assessed by ICP-MS, molar mass of Gd, and molecular weight of polymer. [d]Ionic r_1 determined at 20 MHz. [e]Molecular r_1 was calculated by the equation $r_1 = N \times$ ionic r_1 (where N is the number of Gd) at 20 MHz. The molecular r_1 corresponds to the relaxivity per macromolecule.

Scheme 2. General Procedure for the Preparation of Macromolecular CAs with Various Architectures via a Grafting-To Strategy

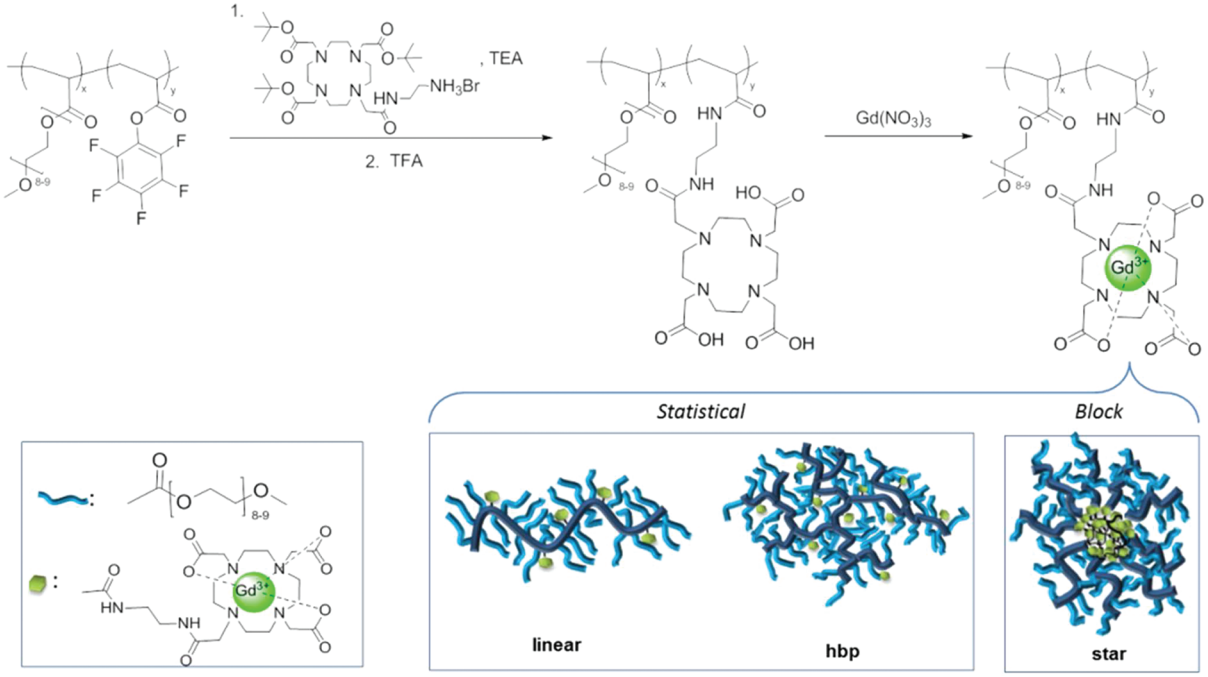

$[RAFT]_0 \times M_w^{PFPA}) + M_w^{RAFT}$, where $[OEGA]_0$, $[PFPA]_0$, and $[RAFT]_0$ stand for initial concentration of OEGA, PFPA, and RAFT agents) and a relatively low dispersity (Table 1).

Synthesis of Star P(OEGA-co-PFPA) Copolymers. The star polymers were synthesized using an arm first approach reported previously by our group.[22] A POEGA homopolymer with M_n = 16 000 g mol^{-1} was prepared by the RAFT polymerization of OEGA at 60 °C over 12 h using AIBN as initiator and 2,2,8-trimethyl-7-oxo-10-thioxo-6-oxa-9,11-dithia-2-silatetradec-3-yn-14-oic acid as CTA. POEGA was then used as a macroCTA to control the copolymerization of PFPA with a cross-linker, *N*,*N*′-bis(acryloyl)cystamine in toluene at 70 °C for 24 h, with a ratio $[PFPA]_0$:$[cross\text{-}linker]_0$:$[POEGA]_0$ of 5:8:1. Under these reaction conditions, where the cross-linker is only partially soluble in toluene, a high incorporation of arms (85.7%, determined by SEC deconvulation, see Supporting Information) occurs yielding low dispersity stars (Table 1 and Figure S22). The residual arms were removed by a long dialysis procedure using a membrane with a molecular cutoff of 50 000 Da yielding pure star polymers. Dynamic light scattering was used to study the sizes and polydispersities of the stars in water. The star polymers were characterized by sizes of around 16 nm with low polydispersities (0.1, measured by DLS, Figure S25B). The molecular weights of the star polymers were calculated from DLS data (M_w = 125 000 g/mol by DLS), allowing us to determine the average number of arms per star from the following equation: $N^{arm} = M_w^{Star}/M_n^{Arm}$. The star structures were found to contain between 7 and 8 arms, i.e., corresponding to around 40 activated ester groups in the core, if all the pentafluoro ester acrylate has been incorporated in the star structure.

A degradable cross-linker was also used in the synthetic procedure with the aim of imparting biodegradability to the stars to aid bioelimination in future *in vivo* studies. To test the potential biodegradability of the star polymers, the polymer dispersed in water was incubated in the presence of glutathione (0.1 M) (a reducing agent naturally present in cells) for 24 h. SEC analysis confirmed that the star polymer dissociated yielding linear arm polymers (Figure S23).

Synthesis of Hyperbranched P(OEGA-co-PFPA) Copolymers. For the hyperbranched polymer synthesis, a one-pot procedure was employed as described by Perrier and co-workers, us, and others.[23] Disulfanediylbis(ethane-2,1-diyl) diacrylate was chosen as a degradable cross-linker with acrylate functionality to minimize potential compositional drift. A copolymerization with a monomer feed ratio of 12.8:3.3:1.6:1.0 (OEGA/PFPA/biodegradable cross-linker/RAFT) was carried out at 60 °C for 12 h. A conversion of 95% in PFPA and 85% in OEGA was attained and no gelation was observed. As in the case of the linear polymer, some compositional drift occurred;

dx.doi.org/10.1021/ma300521c | *Macromolecules* 2012, 45, 4196–4204

however, this was difficult to quantify in the relatively complex branched structure. Analysis of the molecular weight distribution of the hyperbranched structure by SEC showed a relatively high dispersity (M_w/M_n = 1.41, Figure S22), as always observed when using a self-condensing vinyl radical approach to the synthesis of hyperbranched polymers.[24] The size of the hyperbranched polymers was measured by DLS in water, yielding well-defined structures with a size around 8−9 nm (Figure S25A). The molecular weight determined by DLS is 50 000 g/mol. To calculate the number of arms in the hyperbranched structures, the disulfide bridges were cleaved using a reducing agent (glutathione) at 37 °C overnight to yield linear polymers. The linear polymers were analyzed by SEC analysis, confirming a shift from high molecular weight to low molecular (M_n around 8000 g/mol, M_w/M_n = 1.14). The experimental molecular weights of the linear polymers were close to the theoretical values obtained using the following equation: $M_n = \alpha^{OEGA} \times ([OEGA]_0/[RAFT]_0 \times M_w^{OEGA} + \alpha^{PFPA} \times ([PFPA]_0/[RAFT]_0 \times M_w^{PFPA}) + M_w^{RAFT}$, where $[OEGA]_0$, $[PFPA]_0$, and $[RAFT]_0$ stand for initial concentration of OEGA, PFPA, and RAFT agents. In this equation, the mass of the cross-linker was neglected. Using the molecular weight obtained by DLS for the hyperbranched and for the linear polymer obtained by DLS, the number of arms has been estimated to 6−7 arms/per hyperbranched molecule.

Chemical Modification of P(OEGA-*co*-PFPA) Copolymers with DO3A-MA Chelate and Complexation with Gd^{3+}. All P(OEGA-*co*-PFPA) copolymers were modified by reaction with a slight excess of *N*-(2-propionamidoethyl)amine derivative of the chelate 1-tri-*tert*-butyl 2,2′,2″-(1,4,7,10-tetraazacyclododecane-1,4,7-triyl)triacetate (DO3A-*t*Bu) in DMF for 48 h at room temperature (Scheme 2). The reaction was followed by ^{19}F NMR, indicating that all PFPA moieties were converted (Table S1), which was an improvement over the previous work of Grogna et al.[14a] with poly(OEGA-*co*-*N*-acryloxysuccinimide) polymers. It is probable that the higher solubility and reactivity of PFPA moieties, compared with *N*-acryloxysuccinimide, improved the reaction yield. The DO3A-*t*Bu moieties were subsequently deprotected by reaction with trifluoroacetic acid overnight. After evaporation of excess of TFA, the polymers were dialyzed against water over several days. ^1H NMR analysis confirmed that the *tert*-butyl groups were removed successfully (Figures S12, S14, S16, and S18).

The complexation with Gd^{3+} was carried out in an aqueous solution at pH = 8 for 48 h using 1.5 equiv of Gd^{3+} with respect to the DO3A-MA moieties. The final Gd^{3+} contents were determined by ICP-OES. Depending on the polymer architecture, 2.4−6.2 wt % of Gd^{3+} was incorporated in the polymer samples, corresponding to complexation by more than 95% of the chelate moieties (Table S1).

According to DLS measurements and TEM images (Figure 1), the average sizes of the hyperbranched and star CAs were 80 nm (D_h = 82 ± 2 nm, D_{TEM} = 82 ± 10 nm, Figure S25) and 18 nm (D_h = 18 ± 2 nm, D_{TEM} = 15 ± 1 nm, Figure S25), respectively. The size of the hyperbranched increases dramatically from 8 to 82 nm. This increase has been attributed to the self-organization of hyperbranched polymers into more complex architectures in water following the introduction of Gd^{3+} to the structures. In contrast, no significant change has been observed for the linear polymer before and after attachment of Gd^{3+}. With these sizes, renal excretion should be reduced and the blood circulation times of these CAs would be expected to increase (as the size limit for renal excretion is 8 nm).[25]

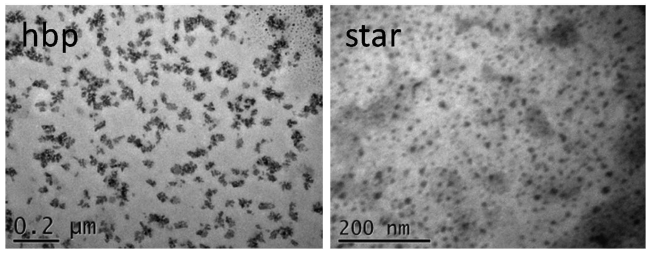

Figure 1. TEM images of hyperbranched and star macromolecular CAs.

Relaxometric Studies. The improvement in contrast promoted by MRI positive CAs is generally measured by the relaxivity (r_1), defined as

$$r_1 = \frac{1}{[Gd^{3+}]}\left(\frac{1}{T_{1,obs}} - \frac{1}{T_{1,H_2O}}\right) \quad (1)$$

where $[Gd^{3+}]$ is the concentration of Gd^{3+} in mM and $T_{1,obs}$ and T_{1,H_2O} are the longitudinal relaxation times in the presence and absence of the MRI CA, respectively. The relaxivity depends on various factors including the external field, the number of coordinated water molecules, water exchange, rotational diffusion, first and second coordination sphere hydration, and the ion to water proton distance.[4a] DOTA-like chelates, such as the DO3A-monoamide used in this work, have a single water molecule coordinated to the Gd^{3+} ion.[4a] Parameters such as the rate of the water exchange (τ_M) and the rotational dynamics of the final molecule (τ_R) are most affected when attaching CAs to a polymer (Scheme 3). Ideally,

Scheme 3. Different Parameters Affecting the Relaxivity of Gd in Water[a]

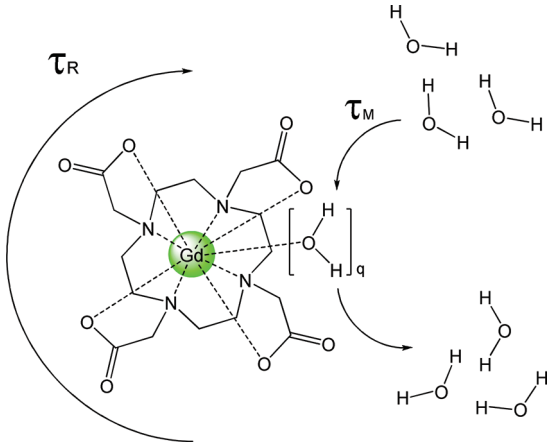

[a] q, τ_M, and τ_R correspond to the number of water coordinate to Gd, rate of water exchange, and the rotational dynamic rate of the final molecule, respectively.

for a small organic contrast agent, τ_M should be at maximum 10 ns and τ_R should be at least higher than 10 ns in a magnetic field of 1.5 T (most commonly used in MRI scanners).[1a]

The results of relaxometric studies at 20 MHz (37 °C) on the P(OEGA-*co*-DO3A-MA-Gd^{3+}) polymers with different architectures (Table 1) indicated an overall increase in

dx.doi.org/10.1021/ma300521c | Macromolecules 2012, 45, 4196−4204

relaxivity compared to the relaxivity of free (no polymer) DO3A-NH$_2$-Gd^{3+} (5.2 mM^{-1} s^{-1}).[14a] This increase is highest for the linear and the hyperbranched architectures, with a relaxivity 3 times higher than the free chelate (Figure 2). The

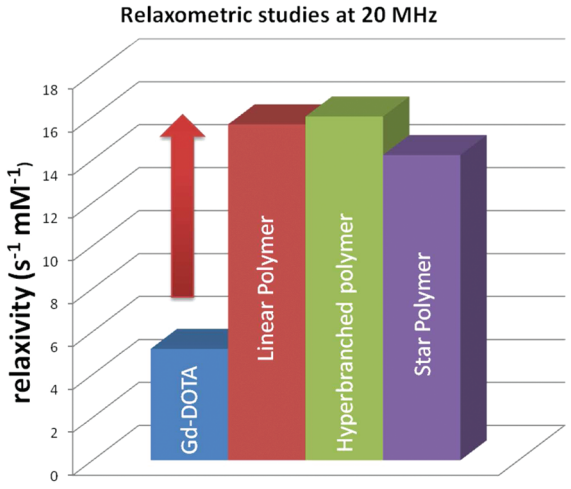

Figure 2. Relaxivity (r_1 at s^{-1} mM^{-1}) of the different polymer architectures.

star polymer showed a slightly lower relaxivity per Gd than the two other polymer architectures. Contrary to expectation, the more globular structure of the hyperbranched polymer did not affect ion relaxivity. In perfectly branched structures, such as dendrimers, the rigid structure imposes a more isotropic rotational dynamics, which strongly increases τ_R and leads to ionic r_1 values in the order of several tens of mM^{-1} s^{-1}.[4c] It seems that the irregular structure of hyperbranched polymers results in a less rigid structure, with relaxivity behavior similar to linear polymer ligands. The self-organization of HPB into larger nanoparticles can have a moderate effect on the relaxivity. Previous studies[9c,26] have shown that the effect of molecular weight of polymers on relaxitivity is relatively low. This indicates that the total hydrodynamic volume of the molecule has less importance than the local mobility of the Gd complex. For instance, in the work of Grogna et al.,[9c] when the micelle size is almost doubled (from 23 to 40 nm), the molar relaxivity remains constant (9.2 mM^{-1} s^{-1}). That is, we suspect that although aggregation is observed, this does not impact the local motion of DO3A-Gd, thus not causing a significant variation of $r_{1,2}$.

However, as hyperbranched polymers have significantly different hydrodynamic radii, they may possess desirable properties for biocirculation and accumulation at tumors. The relaxivity per molecule (or per macromolecule) has been calculated using the following equation: $r_1 = N \times$ ionic r_1 at 20 MHz. Star polymer presents the highest relaxivity/macromolecules compared to the hyperbranched and linear polymers. This value shows that these nano-objects can present a high contrast for a small volume, resulting by a potential higher contrast in MRI.

Figure 3 shows the ^{1}H NMRD profiles of the various macromolecular CAs. A maximum in relaxivity is observed for all the architectures at 40 MHz, which is within the magnetic field range (12.5−125 MHz) used in clinical MRI scanners.

Using the ^{1}H NMRD profiles, we were able to determine the values of τ_M and τ_R by fitting the NMRD profiles for the three different architectures. The star structures did not substantially

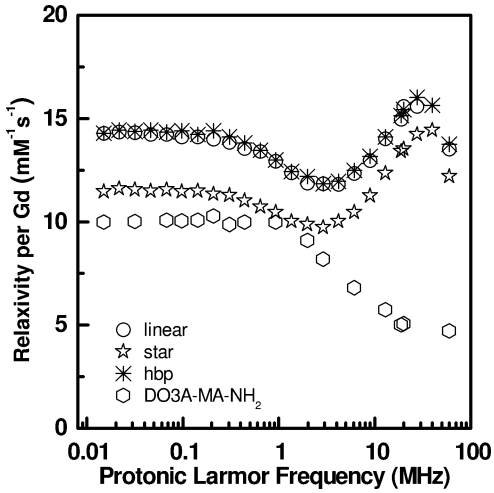

Figure 3. ^{1}H NMRD profiles of P(OEGA-*co*-DO3A-MA-Gd^{3+}) with various architectures.

enhance ionic relaxivity, despite the fact that the Gd^{3+} chelates are held in a rigid environment within the star cores, as indicated by the increase of τ_R (Table 2). An opposing

Table 2. Experimental Values of Rate of the Water Exchange (τ_M) and the Rotational Dynamics of the Final Molecule (τ_R) versus Different Macromolecule Architectures

	linear	HPB	star
τ_M (ns)	691 ± 115	465 ± 98	800 ± 14
τ_R (ps)	555 ± 126	651 ± 84	794 ± 23

influence causing an increase of τ_M has occurred caused by a lack of Gd^{3+} accessibility to surrounding water in the star polymer due to the presence of polymer shell. The polymer shell reduces the diffusion rate of water molecules from the outside to the core and increases the τ_M value compared to hyperbranched polymer and linear polymers (Table 2). To decrease τ_M, the Gd^{3+} ion must efficiently relax the surrounding water molecules, and also, a fast exchange between the relaxed molecule and the bulk water must take place.[4a] This observation is in good agreement with the work reported on the functionalization of dendrimer surface via poly(ethylene glycol) (PEG) polymer; Kobayashi and co-workers[27] have reported that the relaxivity of dendrimer can be decreased by attaching a PEG layer around dendrimer cores. Hyperbranched polymers present the shortest value for τ_M, showing that water molecules can readily access the Gd^{3+} complex (possibly by rapid diffusion to the 3D polymer interior). This result is explicable as the HPB is not a dense and compact polymer structure (contrary to the case of polymer star cores). The rotational dynamic rate in HPB is intermediate between the values obtained from linear (fast rotation) and star polymer (slow rotation), showing that the structure of the HPB is relatively flexible in this case. The value obtained for τ_R corresponds to the values observed in dendrimer structure for generation 1 or 2 in the case polyamidoamine.[16]

However, star architectures may still be useful macroligands, as it is possible to introduce a large number of Gd^{3+} ions per molecule. The number of Gd^{3+} can be easily tuned by varying the concentration of functional groups in the cores. In addition, since the Gd^{3+} ions are located in a more confined

dx.doi.org/10.1021/ma300521c | *Macromolecules* 2012, 45, 4196−4204

environment, the possibility of leakage (and tissue exposure) is reduced even if the blood circulation times are longer.

In-Vitro Studies Using the NIH 3T3 Cell Line: The cytotoxicity of the different macromolecular CAs was investigated using the NIH 3T3 cell line (a common fibroblast cell line) with a Blue Alamar assay. The cytotoxicity of different macromolecule structures (prior to complexation with Gd^{3+}) has been evaluated at different concentrations from 1 to 10 mg/ml of polymers. All these polymers (prior to complexation) are nontoxic (cell viability above 80%, after 3 days). The macromolecular CAs were also evaluated after complexation of Gd^{3+}, confirming nontoxicity for the cell line at Gd^{3+} concentrations below 250 μM (Figure 4). However, above

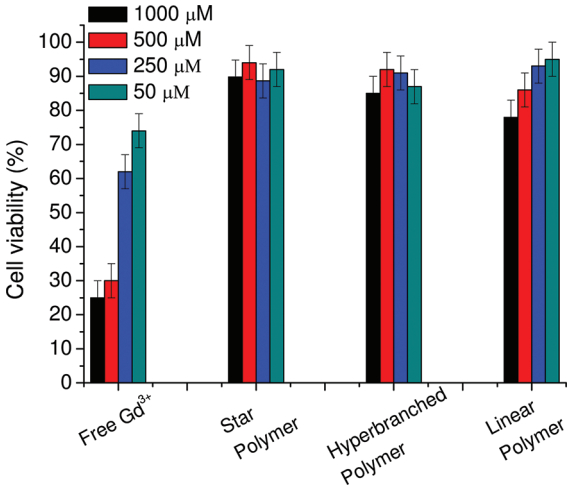

Figure 4. Toxicity study of Gd macromolecule contrast agents using NIH 3t3 cell lines versus the concentration of Gd. Note: all the data have been repeated in triplicate.

Gd concentrations of 250 μM, the linear polymer CA started to display toxicity (in contrast to the star and HPB CAs). We may hypothesize that the complex 3D hyperbranched and star structures increase isolation of Gd^{3+} minimizing cell interactions, thereby negating cytotoxicity. As expected, free Gd^{3+} (without chelating agent) is shown to be cytotoxic even at low concentrations.

CONCLUSION

Complex architectures of P(OEGA-*co*-PFPA) copolymers were synthesized using RAFT polymerization for use as scaffolds to attach Gd^{3+} chelates. In this way, nanoparticles in the range 15−80 nm could be prepared as MRI contrast agents. Relaxivity measurements on the macromolecular CAs demonstrated that linear or hyperbranched polymer structures increased the T_1 relaxation rate and, therefore, would enhance MRI contrast. In contrast, a higher local concentration of Gd^{3+} ions was evident in star-Gd molecules that consequently displayed a much higher molecular relaxivity.

In this paper, we have demonstrated that the architecture plays a crucial role on the different parameters (τ_M (water exchange time) and τ_R (rotational time)) and influx on the relaxivity. Further investigations on the density of the cross-linking and the nature of the cross-linker (rigidity) are in progress to determine the effect on the relaxivity.

In vitro and *in vivo* studies on the macromolecular CAs as well as studies on the biodegradability and elimination of the hyperbranched and star Gd CAs are currently underway. We also plan to introduce targeting moieties to the periphery of the nanoparticle CAs to enhance local contrast effects.

ASSOCIATED CONTENT

Supporting Information

Experimental details, ^{1}H NMR, ^{13}C NMR, and ^{19}F NMR spectra of RAFT agents, cross-linkers, linear polymer arm, hyperbranched and star polymer before and after attachment of DO3A. This material is available free of charge via the Internet at http://pubs.acs.org.

AUTHOR INFORMATION

Corresponding Author

*E-mail: cboyer@unsw.edu.au (C.B.); t.davis@unsw.edu.au (T.P.D.); a.lowe@unsw.edu.au (A.B.L.).

Notes

The authors declare no competing financial interest.

ACKNOWLEDGMENTS

The authors acknowledge the Australian Reseach Council (ARC) for funding in the form of a Discovery grant (DP110104251). In addition, we acknowledge a significant research fellowship funding to C.B. (Australian Postdoctoral Fellowship).

REFERENCES

(1) (a) Hermann, P.; Kotek, J.; Kubicek, V.; Lukes, I. *Dalton Trans.* **2008**, 3027. (b) Werner, E. J.; Datta, A.; Jocher, C. J.; Raymond, K. N. *Angew. Chem., Int. Ed.* **2008**, *47*, 8568. (c) Caravan, P.; Ellison, J. J.; McMurry, T. J.; Lauffer, R. B. *Chem. Rev.* **1999**, *99*, 2293.

(2) (a) Laurent, S.; Forge, D.; Port, M.; Roch, A.; Robic, C.; Vander Elst, L.; Muller, R. N. *Chem. Rev.* **2008**, *108*, 2064. (b) Mahmoudi, M.; Hosseinkhani, H.; Hosseinkhani, M.; Boutry, S.; Simchi, A.; Journeay, W. S.; Subramani, K.; Laurent, S. *Chem. Rev.* **2010**, *111*, 253. (c) Gao, J. H.; Gu, H. W.; Xu, B. *Acc. Chem. Res.* **2009**, *42*, 1097. (d) Na, H. B.; Song, I. C.; Hyeon, T. *Adv. Mater.* **2009**, *21*, 2133.

(3) Perazella, M. A. *Clin. J. Am. Soc. Nephrol.* **2009**, *4*, 461.

(4) (a) Caravan, P. *Chem. Soc. Rev.* **2006**, *35*, 512. (b) Aime, S.; Castelli, D. D.; Crich, S. G.; Gianolio, E.; Terreno, E. *Acc. Chem. Res.* **2009**, *42*, 822. (c) L. Villaraza, A. J.; Bumb, A.; Brechbiel, M. W. *Chem. Rev.* **2010**, *110*, 2921.

(5) (a) Bloembergen, N. *J. Chem. Phys.* **1957**, *27*, 572. (b) Bloembergen, N.; Morgan, L. O. *J. Chem. Phys.* **1961**, *34*, 842. (c) Bloembergen, N.; Purcell, E. M.; Pound, R. V. *Phys. Rev.* **1948**, *73*, 679. (d) Solomon, I. *Phys. Rev.* **1955**, *99*, 559.

(6) (a) Kumar, K.; Chang, C. A.; Francesconi, L. C.; Dischino, D. D.; Malley, M. F.; Gougoutas, J. Z.; Tweedle, M. F. *Inorg. Chem.* **1994**, *33*, 3567. (b) Caravan, P. *Chem. Soc. Rev.* **2006**, *35*, 512.

(7) Adam, G.; Neuerburg, J.; Spüntrup, E.; Mühler, A.; Surg, K. S. V.; Günther, R. W. *J. Magn. Reson. Imaging* **1994**, *4*, 462.

(8) Zarabi, B.; Nan, A.; Zhuo, J.; Gullapalli, R.; Ghandehari, H. *Mol. Pharmaceutics* **2006**, *3*, 550.

(9) (a) Shiraishi, K.; Kawano, K.; Maitani, Y.; Yokoyama, M. *J. Controlled Release* **2010**, *148*, 160. (b) Shiraishi, K.; Kawano, K.; Minowa, T.; Maitani, Y.; Yokoyama, M. *J. Controlled Release* **2009**, *136*, 14. (c) Grogna, M.; Cloots, R.; Luxen, A.; Jerome, C.; Passirani, C.; Lautram, N.; Desreux, J.-F.; Detrembleur, C. *Polym. Chem* **2010**, *1*, 1485.

(10) (a) Kobayashi, H.; Brechbiel, M. W. *Adv. Drug Delivery Rev.* **2005**, *57*, 2271. (b) Langereis, S.; Dirksen, A.; Hackeng, T. M.; van Genderen, M. H. P.; Meijer, E. W. *New J. Chem.* **2007**, *31*, 1152. (c) Nwe, K.; Bryant, L. H.; Brechbiel, M. W. *Bioconjugate Chem* **2010**, *21*, 1014.

(11) Adkins, C. T.; Dobish, J. N.; Brown, C. S.; Mayrsohn, B.; Hamilton, S. K.; Udoji, F.; Radford, K.; Yankeelov, T. E.; Gore, J. C.; Harth, E. *Polym. Chem.* **2012**, *3*, 390.

(12) Bogdanov, A. A.; Weissleder, R.; Frank, H. W.; Bogdanova, A. V.; Nossif, N.; Schaffer, B. K.; Tsai, E.; Papisov, M. I.; Brady, T. J. *Radiology* **1993**, *187*, 701.
(13) Grogna, M.; Cloots, R.; Luxen, A.; Jérôme, C.; Passirani, C.; Lautram, N.; Desreux, J.-F.; Detrembleur, C. *J. Polym. Sci., Part A: Polym. Chem.* **2011**, *49*, 3700.
(14) (a) Grogna, M.; Cloots, R.; Luxen, A.; Jerome, C.; Desreux, J.-F.; Detrembleur, C. *J. Mater. Chem.* **2011**, *21*, 12917. (b) Grogna, M.; Cloots, R.; Luxen, A.; Jerome, C.; Passirani, C.; Lautram, N.; Desreux, J.-F.; Collodoro, M.; De Pauw-Gillet, M.-C.; Detrembleur, C. *Polym. Chem.* **2011**.
(15) (a) Boyer, C.; Bulmus, V.; Priyanto, P.; Teoh, W. Y.; Amal, R.; Davis, T. P. *J. Mater. Chem.* **2009**, *19*, 111. (b) Boyer, C.; Priyanto, P.; Davis, T. P.; Pissuwan, D.; Bulmus, V.; Kavallaris, M.; Teoh, W. Y.; Amal, R.; Carroll, M.; Woodward, R.; St Pierre, T. *J. Mater. Chem.* **2010**, *20*, 255. (c) Boyer, C.; Whittaker, M. R.; Bulmus, V.; Liu, J.; Davis, T. P. *NPG Asia Mater.* **2010**, *2*, 23−30.
(16) Jászberényi, Z.; Moriggi, L.; Schmidt, P.; Weidensteiner, C.; Kneuer, R.; Merbach, A.; Helm, L.; Tóth, É. *J. Biol. Inorg. Chem.* **2007**, *12*, 406.
(17) Boyer, C.; Davis, T. P. *Chem. Comm* **2009**, 6029.
(18) Boyer, C.; Bulmus, V.; Davis, T. P. *Macromol. Rapid Commun.* **2009**, *30*, 493.
(19) (a) Boyer, C.; Bulmus, V.; Davis, T. P.; Ladmiral, V.; Liu, J.; Perrier, S. *Chem. Rev.* **2009**, *109*, 5402. (b) Boyer, C.; Stenzel, M. H.; Davis, T. P. *J. Polym. Sci., Part A: Polym. Chem.* **2011**, *49*, 551.
(20) Eberhardt, M.; Mruk, R.; Zentel, R.; Théato, P. *Eur. Polym. J.* **2005**, *41*, 1569.
(21) Boyer, C.; Whittaker, M.; Davis, T. P. *J. Polym. Sci., Part A: Polym. Chem.* **2011**, *49*, 5245.
(22) (a) Ferreira, J.; Syrett, J.; Whittaker, M.; Haddleton, D.; Davis, T. P.; Boyer, C. *Polym. Chem.* **2011**, *2*, 1671−1677. (b) Syrett, J. A.; Haddleton, D. M.; Whittaker, M. R.; Davis, T. P.; Boyer, C. *Chem. Commun.* **2011**, *47*, 1449.
(23) (a) Luzon, M.; Boyer, C.; Peinado, C.; Corrales, T.; Whittaker, M.; Tao, L.; Davis, T. P. *J. Polym. Sci., Part A: Polym. Chem.* **2010**, *48*, 2783. (b) Liu, B.; Kazlauciunas, A.; Guthrie, J. T.; Perrier, S. *Macromolecules* **2005**, *38*, 2131. (c) Rosselgong, J.; Armes, S. P. *Macromolecules* **2012**, *45*, 2731.
(24) Voit, B. I.; Lederer, A. *Chem. Rev.* **2009**, *109*, 5924.
(25) Soo Choi, H.; Liu, W.; Misra, P.; Tanaka, E.; Zimmer, J. P.; Itty Ipe, B.; Bawendi, M. G.; Frangioni, J. V. *Nat. Biotechnol.* **2007**, *25*, 1165.
(26) Margerum, L. D.; Campion, B. K.; Koo, M.; Shargill, N.; Lai, J.-J.; Marumoto, A.; Christian Sontum, P. *J. Alloys Compd.* **1997**, *249*, 185.
(27) Kojima, C.; Turkbey, B.; Ogawa, M.; Bernardo, M.; Regino, C. A. S.; Bryant, L. H., Jr; Choyke, P. L.; Kono, K.; Kobayashi, H. *Nanomed.: Nanotech., Biol. Med.* **2011**, *7*, 1001.